International Journal of Engineering Trends and Technology
ISSN: 2231 – 5381 /doi:10.14445/22315381/IJETT-V69I12P226
Volume 69 Issue 12, 218-228, December, 2021

Effect of TiO_2, Fe_2O_3, and Duplex of TiO_2 and Fe_2O_3 Fluxes On Microstructural, Mechanical Properties And, Weld Morphology of A-TIG AH-36 Marine-Grade Steel Weldments

K.Vijaya Kumar[1], N. Ramanaiah[2], N. Bhargava Rama Mohan Rao[3]

[1]*Faculty of Mechanical Engineering, GITAM University, Visakhapatnam 530040, India*

[2]*Faculty of Mechanical Engineering, Andhra University College of Engineering, Andhra University, Visakhapatnam 530022, India*

[3]*Faculty of Metallurgical Engineering, Andhra University College of Engineering, Andhra University, Visakhapatnam 530022, India.*

[1]vkalluba@gitam.edu, [2]nalluramanaiah@andhrauniversity.edu.in, [3]nrmrbhargava@rediffmail.com

Abstract *- The current study investigates the metallurgical, mechanical properties and weld morphology of AH-36 marine grade steel with the thickness of 8mm by A-TIG welding butt joints with the application of different fluxes, i.e., TiO_2, Fe_2O_3, and duplex of TiO_2 and Fe_2O_3 at various process parameters, at a constant welding speed 120 mm/min and current varied from 160A to 220A uniformly to optimize process parameters to achieve desired mechanical properties, weld morphology, and lowest possible heat input. The study also focused on comparing tensile strength, impact strength, and microhardness, heat input during welding, and at different operating conditions, weld bead geometry such as Depth (D), width(W), and aspect ratio(D/W) are compared between traditional TIG welding and A-TIG welding. Tensile results reported that fracture occurs at the base region in both TIG welding and A-TIG weldments. The excessive impact strength and irregular heat input were observed with duplex flux coated weldments. A higher aspect ratio, full penetration narrow width of weld bead achieved with TiO_2 and Fe_2O_3 duplex flux coated weldments because of the stable arc, Marangoni effect, and arc constriction. Microhardness results reported that the fusion zone has a higher microhardness in A-TIG welding than ordinary TIG welding. It concluded that TiO_2 and Fe_2O_3 duplex flux coating produced better butt welds of AH-36 steel out of all fluxes. In addition to that, ABAQUS software is used to simulate and validate the tensile test experimental results.*

Keywords *- A-TIG Welding, AH-36 steel, weld bead depth, weld bead width, weld zones.*

I. INTRODUCTION

Tungsten Inert Gas (TIG) welding produces the arc in the middle of a non-consumable Tungsten electrode. The workpieces were welded under a protecting gas environment. Seng et al. [1] propose the TIG welding technique; its high weld quality and considerable weld precession had become the most often used welding method. To weld stainless steel and non-ferrous metals [2] Lin and Wu et al. The TIG welding process makes aircraft components and components for the naval and defense academy. K.H. Tseng and colleagues [3,4] The TIG welding process had a fundamental drawback in that it could only produce a small amount of thick and wide joints. Furthermore, the approximate thickness is to be welded up to 3mm; it demands edge preparation and multi-pass welding after 3mm. According to comparison studies by Sakthivel et al. [5], 3mm full Depth can be achieved in TIG weldments on stainless steel with a single pass. Fujii et al. [6] proposed A-TIG welding to enhance productivity, weld pool depth penetration, and weld shape. Le Conte S et al. [7] noticed that with the aid of an inorganic powder applied to metals before welding termed activating flux, i.e., (TIG), welding limits could be improved. Over the years, many researchers have discovered the use of flux for various arc welding procedures: compared to traditional GTA welding, SiO_2 and TiO_2 produced the most visible effects concerning improving the penetration depth of the weld pool Priya Chauhan et al. [8]. Welding generated by the A-TIG welding process allowed better mechanical characteristics than multi-pass TIG weldments of various steels Sharma. P et al. [9]. Flux also helped integrate and coordinate conventional TIG welding to join larger thick workpieces of 8–12mm using one single pass, avoiding pre-edge preparation and multi-pass welding trials, according to Kuang-Hung Tseng et al. [4]. The A-TIG welding technique's important, appealing qualities were practical arc constriction, high energy densities, low heat consumption, and the impact of angular distortion, according to Sakthivel and Tseng, as well as Kuan. et al. [4,5]. Even though Tseng and Chen. et al. [4] observed that the heat input decreased, and the penetrating ability of GTA welding with TiO_2 flux was enhanced by 240 percent while welding 6mm thick AISI316Lplates. With the activating flux Fe_2O_3,

Kamal H. et al. [10] There was an increase in weld depth and a decrease in weld bead width. Huang et al. [11] applied the A-TIG welding approach with MnO_2–ZnO multi-element flux to investigate the weld bead shape,

held-ferrite contamination, and hot fracture susceptibility of 5mm thick AISI304 workpieces. It also noted many efforts to significantly increase weld depth since this reduces costs and increases GTAW efficiency. Furthermore, in their A-TIG welding experimental findings, Devendranath et al. [12] discovered that employing compound flux SiO_2–TiO_2 had an outsized impact on weld depth as compared to traditional TIG welding under the same conditions. When the Author Hung Tseng et al. [13] compared to the conventional TIG welding method, working with TiO_2 flux on 316L stainless steel workpieces increases weld depth, aspect ratio and decreases weld bead width. The significant restrictions for utilizing GTAW for thick plates are shallow penetration, minimal diffusion, and a poor deposition rate in a single pass Tseng, K. H. and Chen, P. Y et al. [14].

It determined that the penetration depth could be increased by employing activated flux and the creep rupture life. Mechanical characteristics improved, and productivity increased Siddha as well raj Prajapati et al. [15]. However, statistical methods are used to create a formulation based on the percentages of flux components to increase weld depth and mechanical properties. B.G. Paul, Ramesh Kumar, et al. [16]. When comparing the width of the bead on the plate, A-TIG welding creates narrower welds than traditional TIG welding. Full penetration was achieved only with A-TIG welding at 200 A and a 7,8 cm/min speed.MJurica, Z Kožuh et al. [17]. A-TIG welds have better tensile strength than TIG or parent metal welds (618MPa). AbdeljlilHdhibi et al. [18] link this to the development of delta ferrite, which has extraordinarily high mechanical properties.

The A-TIG welding method, which uses flux to aid minimize weld width and promote weld depth, is the technology that has received the most attention. One way often used to improve the industrial efficiency and penetrating ability of the TIG welding process with the use of the addition of flux with the welding process S.A Afolalu and S.B Soetan et.al [19]. In comparison with multi-pass TIG of various steels, A-TIG welding offers superior mechanical properties, Sharma. P and Dwivedi.D et.al [9]. Nineteen compositions were made from three oxides (TiO_2, MoO_3, and SiO_2) using the simplex lattice degree four design, with the best result being 55% TiO_2+45% MoO_3. Compared to standard TIG weld beads, the enhanced formula's depth weld was doubled (7.24 mm) (3.64 mm). Kamel Touileb et.al [20]. Because of Marangoni transformation and arc constriction mechanisms, the A-TIG welding approach achieved the greatest penetration utilizing MoO_3 flux, which is 107 percent greater than a standard TIG weldment. For example, MgO, SiO_2, CaF_2, and $MgCl_2$*$6H_2O$ demonstrated a significant increase in weld penetration Hari Krishna Rana and VishveshBadhekaet al. [21].

The overall goal of this project is to A-TIG welding of AH-36 marine-grade steel and investigate relevant weld morphology and mechanical properties of A-TIG welded joints such as tensile strength, microhardness, and impact strength experimentally. A parametric study has been conducted to predict optimum heat input that indeed yields maximum tensile strength, impact strength, and microhardness of weld joints, in addition to this comparison of TIG and A-TIG weldments with various fluxes such as TiO_2, Fe_2O_3, and duplex of both. The cost practical, time matters, and durability of weld joints for the application of shipbuilding and other marine-related have been studied, and relevant results are presented in the following sections.

II. MATERIAL AND EXPERIMENTAL DETAILS

In the current research, AH-36 steel material was used to perform TIG and A-TIG weldments. The chemical constitution of the workpiece material has been investigated utilizing the dry spectroscopic strategy presented in Table2.

A. Mechanical properties of the workpiece material

The mechanical properties of the workpiece material tested using MAKE-M/S Instron (Model no: 8801)provided in Table 1

III. TABLE 1
BASE MATERIAL MECHANICAL PROPERTIES.

Properties	Value
Yield Strength 0.2%	289.36 Mpa
UTS	453.63 Mpa
Young's Modulus	25.24 Gpa

IV. TABLE 2
THE CHEMICAL CONSTITUTION OF AH36 STEEL MATERIAL CHEMICAL FORM (BY % WEIGHT)

Element	wt.%	Element	wt.%	Element	wt.%	Element	wt.%
C	0.206	Mo	0.00475	Ti	<0.00100	Pb	0.00474
Si	0.262	Cu	0.0264	Zr	<0.00150	As	0.0202
Mn	0.794	Nb	<0.00100	Co	<0.00150	Bi	<0.0040
P	0.00457	V	0.00061	Zn	0.00224	Ce	<0.00300
S	0.0119	W	<0.00100	B	<0.00020	Sb	<0.00100
Cr	0.0521	Ca	0.00169	Al	0.0103	Te	<0.00100
Ni	0.0102	la	<0.00100	Sn	0.00480	Fe	98.600

B. Flux physical properties and appearance

V. TABLE 3
PHYSICAL PROPERTIES OF THE OXIDE FLUXES UTILIZED IN THIS INVESTIGATION [25].

UPAC name of flux	Iron oxide red (Ferric oxide red)	Titanium (IV) oxide
The chemical name for oxide flux	Fe_2O_3	TiO_2
Density (g/cm^3)	5.24	4.23
Molar mass M (g/mol)	159.69	79.90
Melting point temperature (°C)	1566	1843
Boiling point temperature. (°C)	1987	2972
Flux characteristics, applications, and appearance	It's among the three major iron oxides. Fe_2O_3 is ferromagnetic, dark red, and easily damaged by acids. Colour: red-brown, solid, and unscented.	It's also known as Titania. It's used in coatings and adhesives, as well as paper and plastics. Appearance: pristine white, perfumed.

C. Flux weights are estimated by volume to be applied to the weld surface.

The flux was placed in a 5mm width on the wild side of each plate, with a 1mm thickness applied to the whole length of the weld plates shown in Figure 1. The flux volume used on weld plates was 2000 mm3(200×10×1), and all flux volume calculations are presented in Table 4. The weight mass of oxide fluxes used for experimental work was calculated by using the following formula.

Mass(m) = Density(ρ)×Volume(V)

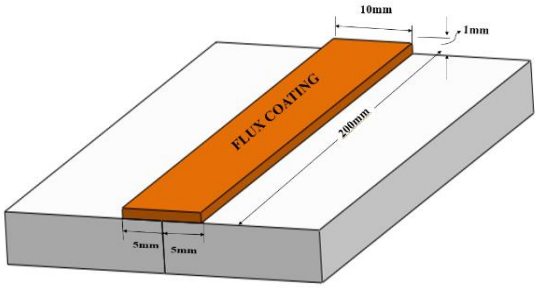

Fig1. Flux volume on to the weld plates

VI. TABLE 4
WEIGHT OF FLUXES CALCULATED ACCORDING TO THE DENSITY AND VOLUME

Type of flux Used	Density (g/cm^3)	Density (g/mm^3)	Volume $(V)mm^3$	Mass in grams(M)
TiO_2	4.23	0.00423	2000	8.46
Fe_2O_3	5.24	0.00524	2000	10.48
Duplex flux of 50%TiO_2 + 50%Fe_2O_3	4.23 & 5.24	0.00423 & 0.00524	1000 + 1000	TiO_2 4.23g + Fe_2O_3 5.24g

C. Tungsten Inert Gas Welding Unit.

TIG Welded joints AH-36 steels with a thickness of 8mm. The butt type of joint is prepared by using the TIG welding technique (Figure 1)

D. Experimental procedure

The current research used hot rolled 8 mm thick AH-36 marine grade steel plates as workpiece materials. By using a water jet machining (WJM) technique, the workpiece material was cut into the desired shape and size, such as rectangular-shaped 200mm×75mm×8mm (Figure 2 illustrates the butt weld setup).

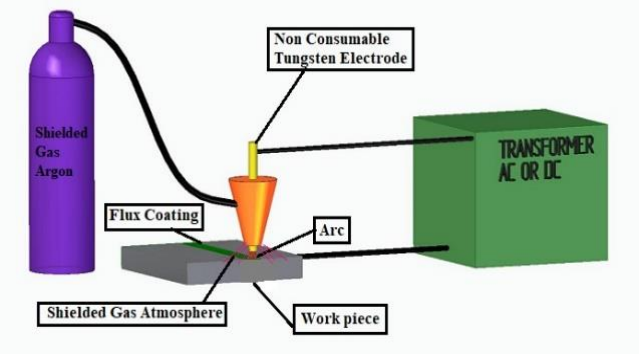

Fig 2. TIG Welding Unit

Once the workpiece materials were cut into the desired shape, a 5mm section was arranged with no gap between workpieces and work surface. The details of the chemical composition analysis of the workpiece material done with a dry spectroscopic approach are provided in Table 1, and the mechanical properties (and value) of the base materials are provided in Table 2. The two workpieces were polished with a surface grinder to remove surface contaminants and were cleaned with acetone. Table 3 shows the oxide fluxes TiO_2, Fe_2O_3, their original form, and physical properties. The mass of fluxes was estimated based on their density and volume (Shown in Figure 1), and it was weighed appropriately presented in Table 4. And TiO_2 and Fe_2O_3 oxide fluxes were combined with acetone in a small cup and stirred with a stirrer. The workpieces were placed in the butt position on the worktable detailed in Figure 3, and the paste-like oxides-acetone mixer was applied on the worktop surfaces of two plates with 5mm width and 1mm thick of each side of the workpieces.

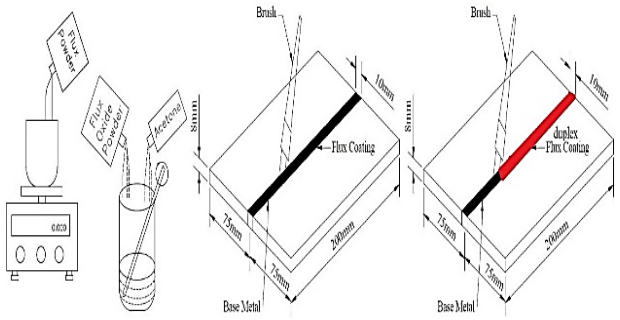

Fig 3. Detailed A-TIG welding Process

According to Ahmadi and Ebrahimi. et al. [22], the activated flux thickness has a significant impact on penetration depth. Tungsten thoriated electrode tip 30˚angle diameter 3mm fitted in a nozzle. Furthermore, Butt welding experiments were conducted with automatic TIG welding equipment using direct current straight polarity (DCSP) power sources. The arc created between the tungsten electrode and the workpiece throughout the process is steady and inert gas shielded (Argon). The process parameters include a constant welding speed of 120mm/min, uniform welding current varying from 160 to 220 amps, and automated voltage changes in response to the current. Then, using water jet machining (WJM), the butt weldments were sliced into various sections to conduct various mechanical testing. Tensile test samples were cut based on the ASTM 8M-04 standards. The Tensile strength of weld joints was determined using a MAKE-M/S Instron (Model no: 8801) with a limit of 100KN and a strain rate of 2 mm/min. Components cut into 50 mm×15 mm×8mm right angle to the welding by keeping the weld area in the center for microhardness estimations and microstructural characterization. The samples were polished using a surface grinding machine and then mechanically ground polished using 1/0, 2/0, 3/0, and 4/0 grade papers, followed by a disc polishing machine using diamond paste as an abrasive medium to ensure a mirror-like image is obtained to reveal the microstructure of components which were etched in a 2% nital solution, followed by cleaning with deionized water and drying with a drier an Inverted Optical microscope (Leica DMILM) used for microstructural characterization. Simultaneously, the composition of the fusion zone was examined using an energy-dispersive X-ray spectroscope (EDS) linked to a scanning electron microscope (SEM) with specifications of 6X to 600000X, detector S.E., BSE, CCD.

E. Tensile test numerical analysis

The tensile test specimens are prepared according to ASTM standards E8M-04 for both base metals as well as flux coated samples as shown in Figure4. Numerical analysis is performed to validate the tensile strength of the experimental results. To validate the experimental results, the Abaqus program is utilized. Mechanical characteristics are filled by the results of experimental tensile tests. To begin the fracturing provided in Table 5, the tensile test numerical model requires a ductile damage material model. Mayank and colleagues [24] used ABAQUS software to simulate tensile tests on CFRP composite material. The tensile strength and stiffness figures agreed well with the experimental result.

Fig 4. Tensile test model ASTM standards E8M-04

V. TABLE 5
TENSILE TEST SIMULATION DUCTILE FRACTURE PARAMETERS

Fracture strain	Stress triaxiality	Strain rate	Displacement at failure
0.45	0.66	0.12	0.5

F. Microhardness TIG and A-TIG weldments

The micro-Vickers hardness number is measured for AH-36 TIG and A-TIG weld joints. The indentation is performed with Equipment G20, which has a maximum capacity of 2kg and provides hardness values directly by measuring the length of the diagonals. It contains microscopes with resolutions of 10X and 40X, allowing us to measure the size of the diagonals. The Vickers hardness (V.H) is determined using the following formula:

$$VHN = 1.854\frac{P}{d^2} \qquad (1)$$

Here the load P is in 'gf,' and the mean diagonal d is in µm (this creates hardness number units of gf/µm2despite the fact that the equivalent units kgf/mm2were chosen; in practice, the numbers are present in place of the units). Different weights and holding durations can be used to perform indentation tests on the specimen. The holding periods are used to determine if the material is dependent on rate-dependent plasticity. For each indentation, measurements were taken in F.Z, HAZ, and P.Z. with a 2Kg weight, 15s dwell duration, and 3mm offsets. Vickers Hardness Number (VHN) measurements were performed on the samples prepared for microstructure observations.

III. RESULTS AND DISCUSSION

A. Impact of flux density on TIG and A-TIG weldment depth of penetration(d), width(w), and aspect ratio (d/w)

The thickness of the flux layer had a considerable influence on the penetration depth of AH-36 steel A-TIG weldments shown in Figure 5. A series of studies discovered that traditional TIG welding generated a wide, narrow depth when the current varied uniformly. At the same time, the other process parameters were kept constant. On the other hand, A-TIG welding under flux applications produced small width and high weld depth. The weld depth grows dramatically as the flux density rises. The weld depth without coating TIG welds or zero thickness coating density correlates to a penetration depth

ranging from 2.20 to 4.04 mm at the tested currents (160 to 220A). At the same process parameters, the weld depth increased from 4.04 mm to 6.21 mm when the flux density ranged from zero to TiO_2 flux density 4.23 g/cm^3. On the other hand, the weld depth ranges from 6.21 to 7.12mm with Fe_2O_3 flux coating A-TIG weldments when the density at the same current credentials varies from 4.23 g/cm3 to 5.24g/cm^3 at the same current credentials. Furthermore, the duplex of 50%TiO_2 and 50% Fe_2O_3 produces Depth ranges from 7.12mm to 8.00mm (complete penetration) for the same process parameters. The results show that weld depth increases as flux density and weld current increase. Similar research by Kamal H. Dhandha, VishveshJ.Badheka et al.[23] found that after the optimal current weld depth becomes constant and decreases.

The above results were that with the application of oxide fluxes, stable arc fluxes and the reverse Marangoni effect were introduced into the weld pool. The weld pool heat moment in TIG welding changed, resulting in various geometrical shapes of weld beads. As TIG welding proceeds, surface tension diminishes along with expanding temperature, pure materials, and alloys. The surface tension of the weld pool mechanism was greater and is extremely low at the edges compared to the weld pool center, especially under the arc. As a result, molten metal moves from the joint middle to the weld pool's boundaries. Due to this mechanism, heat is transferred from the center to the weld boundaries, resulting inwide breadth and reduced weld joint depth. Marangoni transformation is the name of this mechanism. Without flux coating, AH-36 steel weldments with a low aspect ratio (D/W) of around 0.31, a more extended bead width (12.79mm), and little Depth (4.04mm) of weld shapes were achieved in the current research result of Marangoni transformation. The usage of oxide fluxes such as TiO_2, Fe_2O_3, and duplex fluxes, in TIG welding commonly referred to as A-TIG welding.

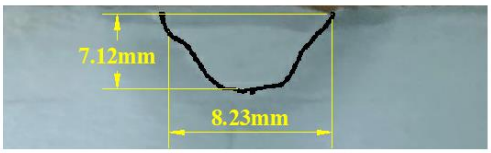

TiO2 flux coating

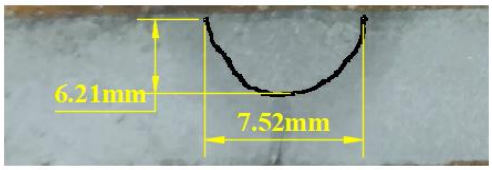

Fe2O3 flux coating

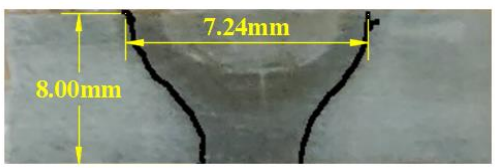

Duplex of TiO2 and Fe2O3 coating

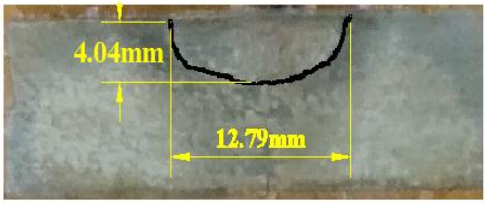

without flux coating

Fig 5. Weld depth variation with different fluxes

These fluxes contain surface-active materials such as oxide components and apply them to the weld surface before welding, which reverses the Marangoni transformation., the flow of molten metal from edges to center; this outcome produces a significant depth of weld joint and less weld joint width. Figure 6 shows the distinctions between Marangoni and reverse Marangoni transformations of TIG and A-TIG welding processes.
With TiO_2 flux A-TIG at optimal current, a weld bead width of 8.23mm and a depth of 7.12mm with

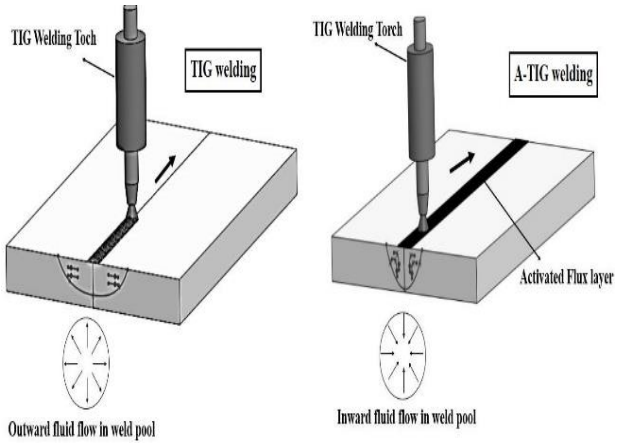

Fig 6.Reverse Marangoni transformation mechanism.

Aspect ratio 1.14. In addition, Fe_2O_3 flux coating width of weld 7.52mm, Depth 6.21mm, and aspect ratio 0.82 at the same process parameters. Finally, the duplex of TiO_2 and Fe_2O_3 flux coated weldments produced full penetration in the weld depth, with a high aspect ratio and narrow weld bead. The above results are much better than the conventional TIG welding. It is advisable to weld with TiO_2 flux because it produces optimum weld bead and aspect ratio. C.R. Heiple reported similar results [25], mainly in stainless steel weld joints. The Depth, width, and aspect ratio variations without flux coated and various flux coated weldments are shown in Figure 7 and Table 6. Suman Saha and Santanu Das et al. [26] found that TiO_2 and Fe_2O_3 fluxes were both capable of lowering penetration shape factor (PFF) (or enhancing aspect ratio); however, TiO_2 is shown to be more effective than Fe_2O_3 flux.

VI. TABLE 6

REPRESENTS WIDTH, DEPTH, AND D/W VALUES AT OPTIMUM CURRENT 220AMP AND WELDING SPEED 120MM/MIN.

Type of Flux	Width(W)in mm	DOP(D) in mm	D/W Aspect Ratio
without flux	12.79	4.04	0.31
TiO_2	8.23	7.12	1.14
Fe_2O_3	7.52	6.21	0.82
TiO_2 and Fe_2O_3 duplex	7.24	8.00	1.06

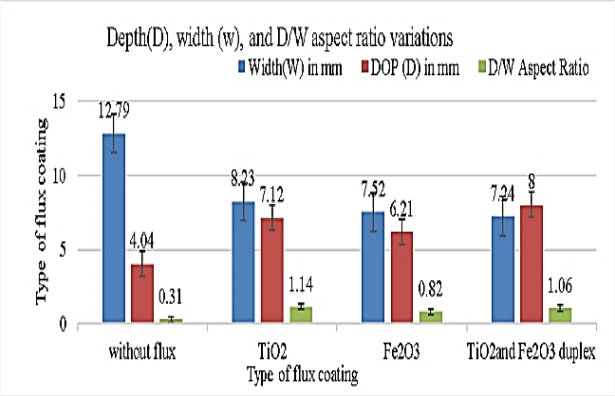

Fig 7. Width, Depth, and D/W variations of TIG and A-TIG weldments

B. Influence of oxide fluxes on heat input of TIG and A-TIG weldments

The current research used direct current straight polarity for all TIG and A-TIG welding experiments.

The following formula can be used to determine heat input

$$\text{Heat Input} = \frac{0.9 \times I \times V \times 60}{1000 \times S} \qquad (2)$$

where V = Arc voltage, I = Arc current, S = welding speed and 0.9 = the arc efficiency [27].

All TIG and A-TIG welding tests had their heat input estimated. It has been observed that the measured arc voltage was growing with an increase in current and the measured heat input proportional to measured arc voltage in ordinary TIG welding as well as TiO_2 and Fe_2O_3 flux coating A-TIG welding weldments shown in Figure 8. TIG welding with flux application considerably increases heat input magnitude during welding, according to research by Hilkes J, Gross V [28]. AccordingtoLeconte S, Paillard P [7], oxides can increase the energy flux density transmitted by the arc to the metal. The current study noticed the heat input for without flux coating weldments higher than the TiO_2 and Fe_2O_3. This is because oxide fluxes supply free electrons to the arc region. As a result, the flow of electrons in the arc area and density of the arc are enhanced. When these electrons strike the work surface, their kinetic energy is converted to heat energy, increasing heat input. The amount of molten metal has always been proportional to the amount of heat energy present. Lu S, Fujii H, and Nogi K [29] found that this resulted in a significant weld depth and a short weld bead width. Because Titanium oxide acts as a slag-producing agent that protects the weld pool from heat loss to the surroundings, so there is no heat transfer from the weld pool to the surroundings during welding with TiO_2 flux. This phenomenon causes the electrical arc's total heat to completely concentrate into the workpiece, resulting in a deep weld bead and excessive heat present in welding. On the other hand, welding using ferric oxides is predicted to release excess oxygen from the weld zone and serve as a shielding gas to protect the wed pool from oxidation, increasing the weld region's heat content, leads higher Depth of the weld. The detected arc voltage in duplex flux coated (50 %t TiO_2 and 50 % Fe_2O_3) A-TIG weldments, on the other hand, has fluctuated with the welding current. Heat intake was first high, then decreased, then increased, owing to significant heat loss to the surroundings. Because the free electron in the flux spills out owing to high-velocity electrons in the arc region as the current increases, the duplex flux achieves high heat input at low current, resulting in intense heat input at high current. Tseng KH, Hsu C-Y et al. [1] conducted a similar study on the initial advantage of utilizing flux to generate high-depth weld beads with the least feasible heat input.

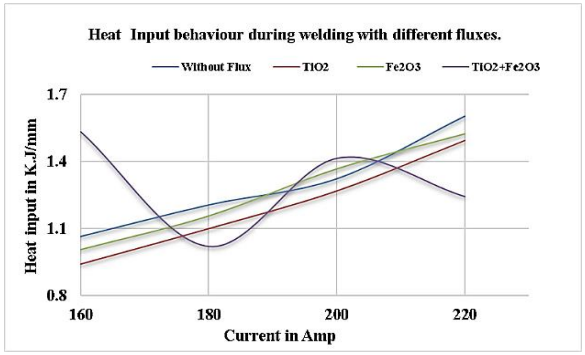

Fig 8.The heat input behavior of TIG and A-TIG weldments at different currents.

C. Effect of TiO_2, Fe_2O_3, and duplex of TiO_2+Fe_2O_3 fluxes on tensile strength of weld joints

Tensile tests were conducted on Instron Model No: 8801 for weldments prepared by various fluxes at different currents and voltage, welding sped maintained constant. All the weldments fracture occurs at the parent zone.

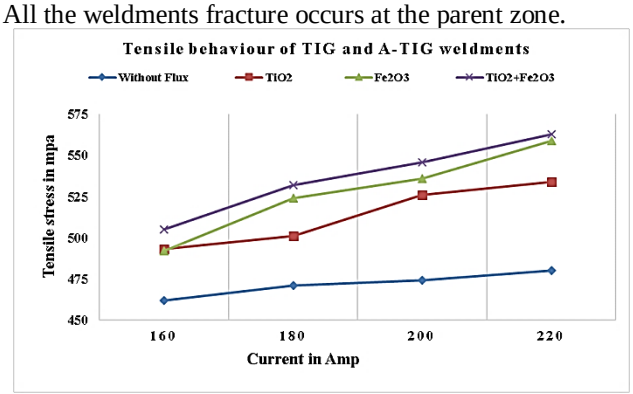

Fig 9.Variation in tensile stresses at various currents of different fluxes

The mean tensile strength of TIG and A-TIG welding results are shown in Figure 9 at different currents compared to TiO_2, Fe_2O_3, and duplex (50% TiO_2 and 50% Fe_2O_3) flux coated A-TIG weldments; conventional TIG weldments produce low tensile strength in all trails. In addition, as compared to the base material, conventional TIG and A-TIG weldments generated high tensile strength in all experiments. In addition, Figure 9 also reveals that the tensile behavior of A-TIG weldments is higher than in the TIG welding experiments. However, the tensile strength of traditional TIG weldments is closer to the parent material. The current research concludes optimum condition to weld AH-36 steel at 220amp,120mm/min welding speed with duplex flux, which provides high tensile strength 563Mpa. Besides, Fe_2O_3 and TiO_2 flux-coated A-TIG weldments produce higher tensile strength than TIG weldments at the same parameters. The SEM-EDS findings in the weld region of conventional TIG weldments are shown in Figure 10; a few other alloying elements, such as Al, Si, Ca, P, and Mn, will also be shown in the weld pool. However, they have little effect in increasing the tensile strength of weldments. Under varied circumstances, the whole weld area melts and cools at room temperature at a non-uniform rate. As a result, compared to the parent material, the tiny grain structure achieved in the fusion region leads to high strength.

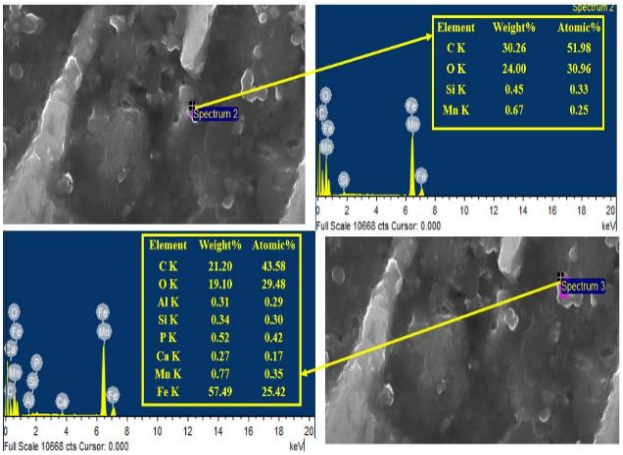

Fig 10. SEM-EDX results of the Fusion zone and

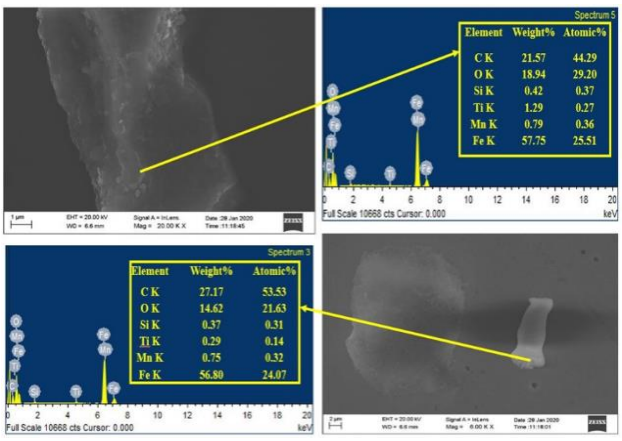

Fig 11. SEM-EDS results of Fusion with TiO_2 flux coating.

Figure 11 shows SEM-EDS, TiO_2 Flux coated A-TIG weldment fusion zone at 220A, 120mm/min welding speed. In that, 1.29% of titanium in the weld pool serves as an alloying element and leads to solid pearlite production; as a result, the strength of the weld joint is enhanced. During welding with Fe2O3 flux coating, iron separates from the oxide and combines with the steel, increasing the strength of the steel since iron content dominates steel strength. Figure 12 SEM-EDS shown that of Fusion with Fe_2O_3 flux coating reveal that 53.80% of the weld area's iron is present, compensating for the high strength of Fe_2O_3 flux coating weldments. The weld strength was found to be greater than that of the base metals in the current investigation. A higher quantity of pearlite and a modest amount of ferrite could explain the higher tensile strength. The increased tensile strength might be attributed to the titanium dissolved in the pearlite phase having a solid solution strengthening effect, making it stronger. Similar findings were reported by Sakthivel and Vasanth raja et al. [5],[30].

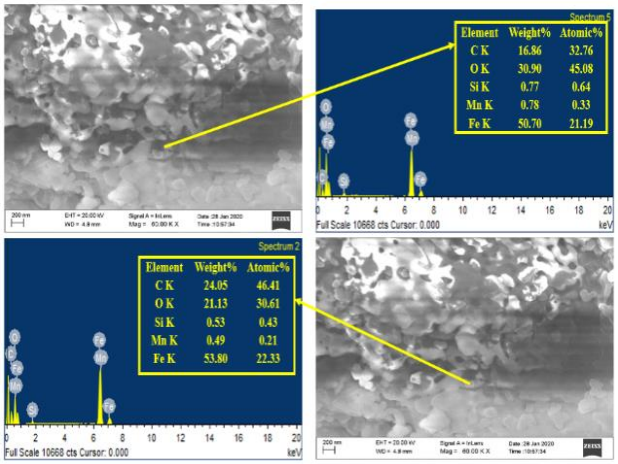

Fig 12. SEM-EDS results of Fusion with Fe2O3 flux coating

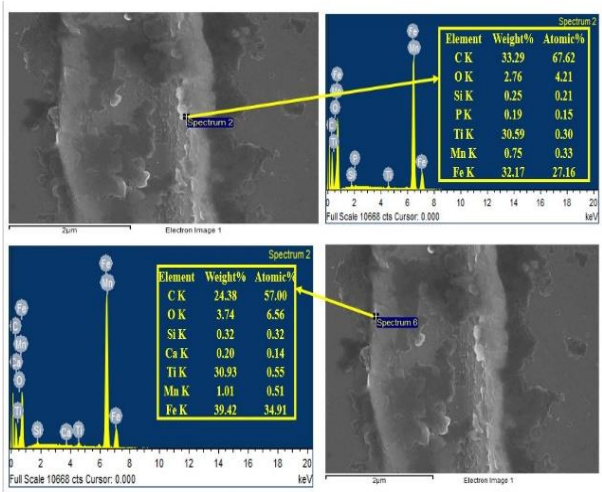

Fig 13. SEM-EDAX results of Fusion with TiO_2 and Fe_2O_3 duplex flux coating

Finally, the tensile results of duplex flux (50% TiO_2 and 50 % Fe_2O_3) weldments reveal strong tensile strengths in all trails, which is predicted given that SEM-EDS findings Figure 13 Ti (30.93%) and Fe (39.42%) play key alloying elements in the strength increase. It is recommended to proceed welding with duplex flux at 220A current and 120mm/min to obtain high tensile strength.

D. Comparison of numerical and experimental tensile results of TIG and A-TIG weldments

Tensile strength of AH-36 steels with TiO_2+Fe_2O_3 duplex flux coating, AH-36 steel with Fe_2O_3 flux coating, and AH-36 steel with TiO_2 flux coating is 17.29 %, 16.4%, 11.25%, respectively higher than the base metal (AH-36 steel) without coating. Comparative studies are done by doing the numerical tensile test analysis. Tensile strength obtained with numerical analysis has a maximum 3.10 % deviation as compared to the experimental result. Numerical analysis shows reasonable justification with the practical effect, as shown in Table 7. Numerical tensile test fractured sample is matching with experimental tensile test fractured samples, as shown in Figure 14 a and e without flux, coated, b and f TiO_2 flux coated, c and g Fe_2O_3 flux coated, d and h duplex flux coated fractured tensile test experimental and numerical simulated welded samples. D Yu et al. [31] compared the experimental tensile test data with numerical simulation and found that numerical analysis had given the accurate result of tensile result and stress-strain curve.

VII. TABLE 7
TENSILE STRENGTH OBTAINED FROM EXPERIMENTAL AND NUMERICAL ANALYSIS AT 220A AND 120MM/MIN PERFORMED WELD JOINTS.

Material	Experimental Tensile strength in Mpa	Computational Tensile strength in Mpa	% Error
Base metal (AH-36 steel) without flux coating.	480	495	3.10
AH-36 steel with TiO_2 flux coating.	534	545	2.05
AH-36 steel with Fe_2O_3 flux coating	559	575	2.86
AH-36steel with TiO_2+Fe_2O_3 duplex flux coating	563	579	2.84

Fig14. Experimental and simulated tensile test samples

E. Effect of TiO_2, Fe_2O_3 and duplex of TiO_2+Fe_2O_3 fluxes on Impact energy of weld joints

A Charpy I-Zod impact test was done at room temperature without flux coating weldments and TiO_2, Fe_2O_3 flux, and duplex of TiO_2+Fe_2O_3 flux A-TIG weldments. The V-Notch is positioned in the fusion zone to determine the fusion zone impact energy. The findings of the experiments show that the impact energy is more significant in all flux-coated A-TIG weldments. Duplexes of TiO_2+Fe_2O_3, on the other hand, have a more substantial impact on energy. Figure 15 shows the impact energy distribution of TIG and A-TIG weldments in TiO_2, Fe_2O_3, and duplex TiO_2+Fe_2O_3 conditions.

VIII. TABLE 8
IMPACT STRENGTH OBTAINED FROM EXPERIMENTAL WITHOUT AND WITH FLUX-COATED A-TIG WELDMENTS

Type of Flux Coating	Current Amp			
	160	180	200	220
Without Flux Coating	1.281	1.658	1.906	1.962
TiO_2	1.464	1.854	2.354	2.543
Fe_2O_3	1.573	1.749	2.471	2.462
Duplex of TiO_2+Fe_2O_3	1.683	1.964	2.511	2.532

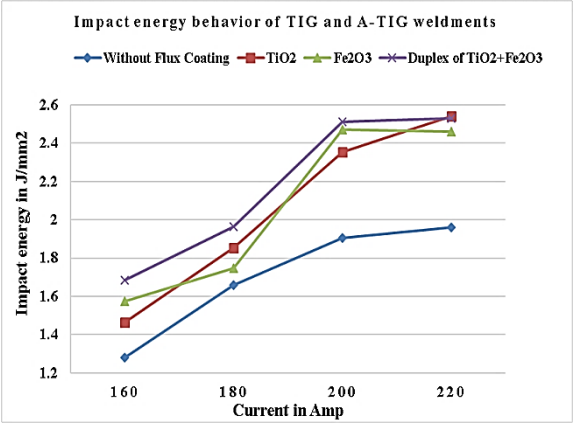

Fig 15.Impact energy behavior of TIG and A-TIG weldments under TiO_2, Fe_2O_3 and duplex TiO_2+Fe_2O_3

It is observed from Figure 15 that duplex flux coated weldments attains high impact energy other than TIG and TiO_2, Fe_2O_3 flux coated A-TIG weldments. This is because the fusion zone cooled at room temperature during welding, resulting in bainite structure and maintained austenite structure shown in Figure16. This results in increased resistance to impact loads. Furthermore, SEM-EDS data is shown in Figure 13. Ti (30.93%) and Fe (39.42%) play key alloying elements, resulting in the formation of solid pearlite, which increases the strength of the weld joint. On the other hand, iron 53.80 % is present in the weld zone, which increases the resistance to impact loads, similar results reported by Kamel Touileb, AbousoufianeOuis et al. [32].

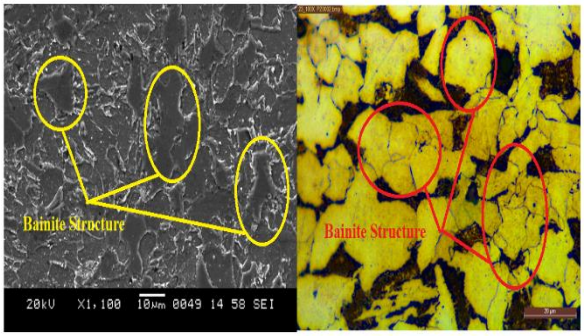

Fig 16.Bainite structure in the fusion zone of duplex coated weldment

F. Effect of fluxes on microhardness of F.Z., HAZ, and P.Z. of TIG and A-TIG weldments

Among all fluxes, greater microhardness was obtained Fe_2O_3 flux coat A-TIG weldments approximately 294VHN at process parameters of 220Amp current and welding speed 120mm/min, according to microhardness study findings. At the same process parameters, flux-coated weldments were shown to have a greater hardness than conventional TIG weldments. Figure 17 indicates that Microhardness values without flux coated weldments in the fusion zone are lower than flux coating and duplex flux coating about 243VH (F.Z.). Similar results were obtained using TiO_2 for 250VHN and 262VHN, as well as duplex flux-coated weldments. Furthermore, All Fusion Zone Micro Hardness values with and without flux coating weldments are higher than the heat-affected zone and parent Zone. The reason behind this, From Figure18 it is that the fusion zone has an equiaxed grain structure; as a result, it achieved the highest microhardness values among all three zones.

On the other hand, the parent region has a coarse grain structure because it possesses less hardness. It also observed that HAZ has a fine grain structure; this leads to microhardness values fluctuating between P.Z. and F.Z. values. Similar reported by K. Devendra Nath Ramkumar et al. [12].

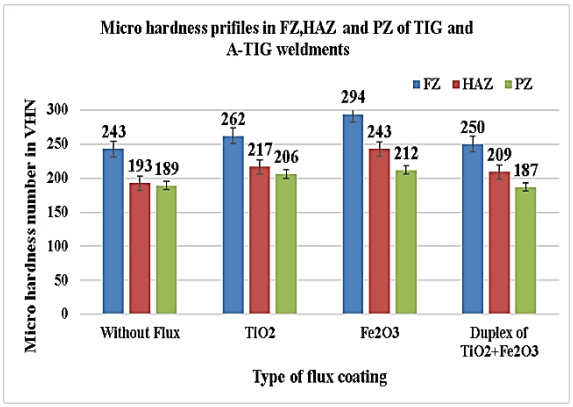

Fig 17. Microhardness values of with and without flux coated and duplex flux weldments of F.Z., HAZ, and P.Z

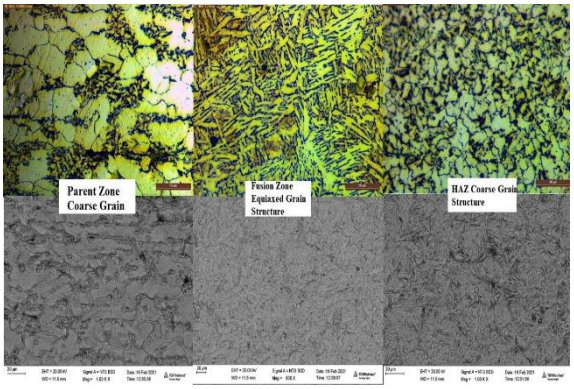

Fig 18.Microstructure variation in P.Z., F.Z., and HAZ in the weld portion

IV. CONCLUSIONS

The current study experiments led and examined TIG welding using oxide flux before the welding of two AH-36 steel plates in the butt position. The fluxes are utilized as follows TiO_2,

Fe_2O_3, and TiO_2 and Fe_2O_3 duplex flux. The principal results got and summed up as follows:

1. Inadequate high calibre and better appearance of the surface acquired of AH-36 steel weldments with Activated flux and duplex flux TIG welding process.
2. Higher weld penetration depth accomplished of the weld joint with the use of duplex flux(8.45mm), TiO_2(7.12mm), and Fe_2O_3 (6.21mm) fluxes, and these higher than the conventional TIG weldments.
3. The purpose behind the higher Depth of penetration was the impact of Marangoni transformation, stable arc, and arc constriction choking resulting from oxide fluxes.
4. The heat input results noticed a significant increase due to the usage of oxide fluxes. Up to this time, the activated flux coating TIG welding process could enhance the electric arc voltage. A weld's heat input per unit length is likewise considerably increased. Hence, the delta-ferrite amount in the weld region material could be enhanced. However, in addition to that, usage of oxide flux coating on work surfaces before welding does not significantly impact the hardness of welded joints.

5. The A-TIG welding method can Increase the welds Depth to width ratio and ensure the greatest duplex flux (1.920) and TiO_2 change (1.142) compared with the traditional TIG welding method.
6. The Mechanical properties of A-TIG welded AH-36 weldments predominant than the normal TIG welding process.
7. Considering all fluxes experimental trails, duplex flux is effectively used to weld AH-36 steel 8mm thick plates in Butt position at 220Amp current and 120mm/min process parameters.
8. In this study, the microstructure considers showing that columnar structure and equiaxed in the fusion zone using oxide fluxes, which drives predominant mechanical properties than the ordinary TIG welding.
9. Numerical analysis error for the tensile test is 3.10%, which shows good agreement with the experimental result.

ACKNOWLEDGMENTS

Acknowledgments The author is grateful to the Indian Institute of Technology Madras, India, for coming up with an opportunity to conduct practical work required for the research. Hindustan Shipyard Pvt Ltd (HSL), Visakhapatnam, India, for sponsoring the raw material for research works, and GITAM University Visakhapatnam, India, for their support for conducting experimental work analysis.

REFERENCES

[1] Tseng KH, Hsu CY. Performance of activated TIG process in austenitic stainless-steel welds. Journal of Materials Processing Technology 211 (2011) 503–512. DOI: 10.1016/j.jmatprotec.2010.11.003.

[2] Lin HL, Wu TM. Effects of activating flux on weld bead geometry of Inconel 718 alloy TIG welds. Materials Manufacturing Process 27(12) 1457–1461:DOI: org/10.1080/10426914.2012.677914

[3] Tseng K, Chuang K. Application of iron-based powders in tungsten inert gas welding for 17Cr–10Ni–2Mo alloys. Powder Technology 228 (2012) 36-46.DOI:10.1016/j.powtec.2012.04.047

[4] Tseng K.H, Chen K.L. Comparisons between TiO_2- and SiO_2-flux assisted TIG welding processes. Journal of Nanoscience and Nanotechnology 12(8) (2012) 6359-67. DOI: 10.1166/jnn.2012.6419

[5] Sakthivel. T et al. Comparing creep-rupture behavior of type 316L (N) austenitic stainless-steel joints welded by TIG and activated TIG welding processes.Materials Science Engineering, 528(22) (2011) 6971– 6980. DOI: 10.1016/j.msea.2011.05.052.

[6] Fujii H, Sato T, Lu S, Nogi K. Development of an advanced A-TIG (AA-TIG) welding method by control of Marangoni convection. Materials Science Engineering 495(1) (2008) 296–303. DOI:10.1016/j.msea.2007.10.116

[7] Le Conte S, Paillard P, Chapelle P, HenrionG, Saindrenan.J. Effect of oxide fluxes on activation mechanisms of tungsten inert gas process. Science and Technology of Welding and Joining 11(4) (2006) 389–397:doi.org/10.1179/174329306X129544.

[8] Priya Chauhan, Hemant Panchal A Review On Activated Gas Tungsten Arc Welding(A-GTAW), International Journal of Science & Engineering Development Research (www.ijsdr.org), ISSN:2455-2631, 1(5) (2016) 798 - 803, Available: http://www.ijsdr.org/papers/IJSDR1605145.pdf

[9] Sharma, P.; Dwivedi, D. K. Comparative Study of Activated Flux-GTAW and Multipass-GTAW Dissimilar P92 Steel-304H ASS Joints. Material Manufacturing Process. (2019). DOI: 10.1080/ 10426914.2019.1605175.

[10] Kamal H. Dhandha, Vishvesh J. Badheka, Effect of activating fluxes on weld bead morphology of P91 steel bead-on-plate welds by flux assisted tungsten inert gas welding process. Journal of Manufacturing Processes, 17 (2015) 48-57.DOI:10.1016/j.jmapro.2014.10.004.

[11] Huang HY, Shyu SW, Tseng KH, Chou CP. Evaluation of TIG flux welding on the characteristics of stainless steel. Science and Technology of Welding and Joining 10(5) (2005) 566–73.doi.org/10.1179/174329305X48329.

[12] Devendra Nath Ramkumar, Jelli Lakshmi Narasimha Varma, Gangineni Chaitanya, Ayush Choudhary, N. Arivazhagan,S. Narayanan. Effect of autogenous GTA welding with and without flux addition on the microstructure and mechanical properties of AISI904L joints. Materials Science & Engineering A636 (2015) 1–9. DOI:10.1016/j.msea.2015.03.072.

[13] Kuang-Hung Tseng, Development, and application of oxide-based flux powder for tungsten inert gas welding of austenitic stainless steels, Powder Technology, 233 (2013) 72-79. http://dx.doi.org/10.1016/j.powtec.2012.08.038

[14] Tseng, K. H, Chen P. Y. Effect of TiO_2 Crystalline Phase on Performance of Flux Assisted GTA Welds. Materials and Manufacturing Processes 31(3) (2016) 359–365.https://doi.org/10.1080/10426914.2015.1058952.

[15] Prajapati S, Shah K. Experimental Study on Activated Tungsten Inert Gas Welding-A review paper. International Journal of Advance Research and Innovative Ideas in Education 2(3) (2016) 2555-2559.

[16] Paul BG, Ramesh Kumar KC. Effect of single component and binary fluxes on the depth of penetration in a-TIG welding of Inconel alloy 800H austenitic stainless steel. International Journal of Advanced Engineering and Global Technology 5 (2017) 1791–1795. https://doi.org/10.48084/etasr.2097

[17] Jurica M, Kozuh Z. Optimization of the A-TIG welding for stainless steels.IOP Conference Series: Materials Science and Engineering; 329, 2018. IOP Conf. Series: Materials Science and Engineering 329 (2018) 012012. doi:10.1088/1757-899X/329/1/012012

[18] Hdhibi A, Touileb K, Djoudjou R, Ouis A, Bouazizi ML, Chakhari J. Effect of Single Oxide Fluxes on Morphology and Mechanical Properties of ATIG on 316 L Austenitic Stainless-Steel Welds. Engineering, Technology & Applied Science Research 8(3) (2018) 3064-3072,.https://doi.org/10.48084/etasr.2097.

[19] Afolalu SA, Soetan SB, Ongbali SO, Abioye AA, Oni AS. Impact of activated–flux tungsten inert gas (A-TIG) welding on weld joint of a metal-Riew. Materials Science and Engineering; IOP Conf. Series: Materials Science and Engineering 640 (2019) 012064. doi:10.1088/1757-899X/640/1/012064

[20] Touileb K, Ouis A, Djoudjou R, Hedhibi A-C, Alrobei H, Albaijan I. Effects of A-TIG welding on weld shape, mechanical properties, and corrosion resistance of 430 ferritic stainless-steel alloy.Metals 10(3) (2020) 404; https://doi.org/10.3390/met10030404.

[21] Rana H, Badheka V, Patel P, Patel V, Li W, Andersson J. Augmentation of weld penetration by flux assisted TIG welding and its distinct variants for oxygen-free copper. Journal of Materials Processing Technology 10 (2021) 138–151. https://doi.org/10.1016/j.jmrt.2020.12.009

[22] Ahmadi E, Ebrahimi AR. Welding of 316L Austenitic Stainless Steel with Activated Tungsten Inert Gas Process.Journal of Materials Engineering and Performance 24 (2014) 1065–1071. DOI:10.1007/s11665-014-1336-6.

[23] Kamal H. Dhandha, Vishvesh J. Badheka, Effect of activating fluxes on weld bead morphology of P91 steel bead-on-plate welds by flux assisted tungsten inert gas welding process, Journal of Manufacturing Processes, 17 (2015) 48-57. http://dx.doi.org/10.1016/j.jmapro.2014.10.004.

[24] Mayank Nirbhay, Anurag Dixit, R.K. Misra, Harlal Singh Mali, Tensile Test Simulation of CFRP Test Specimen Using Finite Elements, Procedia Materials Science, 5 (2014) 267-273. doi: 10.1016/j.mspro.2014.07.266.

[25] Heiple CR and Roper JR. ASM Conf. Trends in Welding Research in the United States, New Orleans, LA, 1982 (1981) 489–515.

[26] Suman Saha[1]and SantanuDas[2] Effect of polarityandoxide fluxes on weld-bead geometry in activated tungsten inert gas (A-TIG) weldingJournal of Welding and Joining, 38(4) (2020) 380-388 https://doi.org/10.5781/JWJ.2020.38.4.7

[27] Arivazhagan B, Vasudevan M. A study of microstructure and mechanical properties of grade 91 steel A-TIG weld joint.Journal of

Materials Engineering and Performance 22(12) (2013) 3708–3716. DOI: 10.1007/s11665-013-0694-9

[28] Hilkes J, Gross V. Welding Cr-Mo steels for power generation and petrochemical applications – past, present, and future.BiulInstytSpawalnictwa 2(1) (2013) 1–22.

[29] Lu S, Fujii H, Nogi K. Marangoni convection and weld shape variations in Ar–O2 and Ar–CO_2 shielded GTA welding. Materials Science Engineering 2004; 380:290–297

[30] Vasantharaja P, Vasudevan M. Studies on A-TIG welding of low activation ferritic/martensitic (LAFM) steel. Journal of Nuclear Materials 421 (2012) 117–123. 10.1016/j.jnucmat.2011.11.062

[31] Yu, D. N., Wang, Y., & She, J. W., Simulation of Metal Material Quasi-Static Tensile Test Based on ABAQUS. Applied Mechanics and Materials, 328 (2013) 985–989.

[32] Kamel Touileb 1, AbousoufianeOuis 1 Effects of ATIG Welding on Weld Shape, Mechanical Properties, and Corrosion Resistance of 430 Ferritic Stainless-Steel Alloy, MDPI journals, Metals, 10 (2020) 404. doi:10.3390/met10030404.